Title

Evaluating the risk of phosphorus loss with a distributed watershed model featuring zero-order mobilization and first-order delivery

Authors

Li, Sisi

Zhang, Liang

Liu, Hongbin

et al.

Publication Date

2017-12-01

DOI

10.1016/j.scitotenv.2017.07.173

Peer reviewed

Science of the Total Environment 609 (2017) 563–576

Contents lists available at ScienceDirect

Science of the Total Environment

journal homepage: www.elsevier.com/locate/scitotenv

Evaluating the risk of phosphorus loss with a distributed watershed model featuring zero-order mobilization and first-order delivery☆,☆☆,★

Sisi Li [a], Liang Zhang [a,*], Hongbin Liu [b,c,**], Hugo A. Loáiciga [d], Limei Zhai [b,c], Yanhua Zhuang [a], Qiuliang Lei [b,c], Wanli Hu [e], Wenchao Li [b,c], Qi Feng [a], Yun Du [a]

[a] Institute of Geodesy and Geophysics, Chinese Academy of Sciences, Wuhan 430077, China
[b] Institute of Agricultural Resources and Regional Planning, Chinese Academy of Agricultural Sciences, Beijing 100081, China
[c] Key Laboratory of Nonpoint Source Pollution Control, Ministry of Agriculture, Beijing 100081, China
[d] Department of Geography, University of California, Santa Barbara, California 93106, USA
[e] Institute of Agricultural Environment and Resources, Yunnan Academy of Agricultural Sciences, Kunming 650205, China

HIGHLIGHTS

- Simulate phosphorus loss processes across landscape as storage-mobilization-delivery
- Grid-based travel time along flow paths considered in phosphorus delivery process
- Spatially distributed results for identifying sub-field critical source areas
- Model results facilitate the selection, design and placement of management practices.

GRAPHICAL ABSTRACT

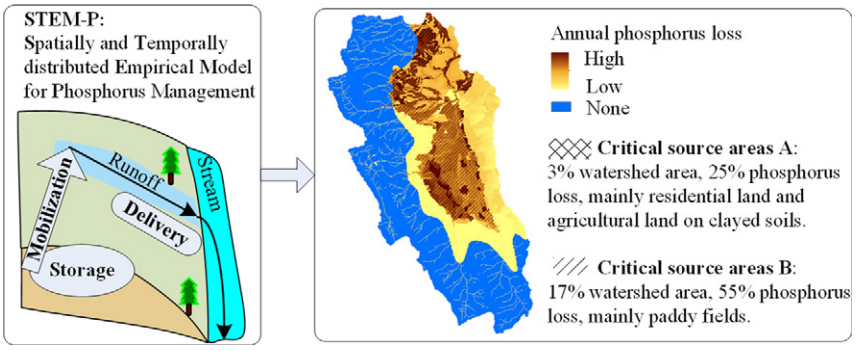

ARTICLE INFO

Article history:
Received 22 April 2017
Received in revised form 12 July 2017
Accepted 20 July 2017
Available online 27 July 2017

Keywords:
Non-point source pollution
Phosphorus
Mobilization
Delivery
Critical source areas
Flow path

ABSTRACT

Many semi-distributed models that simulate pollutants' losses from watersheds do not handle well detailed spatially distributed and temporal data with which to identify accurate and cost-effective strategies for controlling pollutants issuing from non-point sources. Such models commonly overlook the flow pathways of pollutants across the landscape. This work aims at closing such knowledge gap by developing a Spatially and Temporally Distributed Empirical model for Phosphorus Management (STEM-P) that simulates the daily phosphorus loss from source areas to receiving waters on a spatially-distributed grid-cell basis. STEM-P bypasses the use of complex mechanistic algorithms by representing the phosphorus mobilization and delivery processes with zero-order mobilization and first-order delivery, respectively. STEM-P was applied to a 217 km^2 watershed with mixed forest and agricultural land uses situated in southwestern China. The STEM-P simulation of phosphorus concentration at the watershed outlet approximated the observed data closely: the percent bias (P_{bias}) was −7.1%, with a Nash-Sutcliffe coefficient (E_{NS}) of 0.80 on a monthly scale for the calibration period. The P_{bias} was 18.1%, with a monthly E_{NS} equal to 0.72 for validation. The simulation results showed that 76% of the phosphorus load was transported with surface runoff, 25.2% of which came from 3.4% of the watershed area (classified

☆ The submission is from the 1st International Conference on Ecotechnologies for Controlling Non-point Source Pollution and Protecting Aquatic Ecosystem (ENPE2017).
☆☆ The abstract ID for ENPE2017 is No. 68.
★ Registration Numbers: Sisi Li, ENPE2017-123; Liang Zhang, ENPE2017-142; Yanhua Zhuang, ENPE2017-211, Qi Feng, ENPE2017-217.
* Corresponding author.
** Correspondence to: H. Liu, Institute of Agricultural Resources and Regional Planning, Chinese Academy of Agricultural Sciences, Beijing 100081, China.
E-mail addresses: lzhang@whigg.ac.cn (L. Zhang), liuhongbin2002@126.com (H. Liu).

http://dx.doi.org/10.1016/j.scitotenv.2017.07.173

as standard A critical source areas), and 55.3% of which originated from 17.1% of the watershed area (classified as standard B critical source areas). The standard A critical source areas were composed of 51% residences, 27% orchards, 18% dry fields, and 4% paddy fields. The standard B critical source areas were mainly paddy fields (81%). The calculated spatial and temporal patterns of phosphorus loss and recorded flow pathways identified with the STEM-P simulations revealed the field-scale critical source areas and guides the design and placement of effective practices for non-point source pollution control and water quality conservation.

1. Introduction

Water-quality deterioration caused by excessive nutrient discharge has been widely documented (Davis and Koop, 2006; Ma et al., 2011; Novotny, 1999; Smith, 2003). Non-point source (NPS) pollution is identified as a leading environmental threat. The control of water pollution by non-point sources of nutrients remains a challenge for scientists and managers since the processes of pollution storage, mobilization, and delivery are complex. Accurate and cost-effective pollution control and sustainable watershed management require detailed information on (1) reliable estimation of pollution load, (2) reliable identification of critical source areas (CSAs) (Chen et al., 2013; Shen et al., 2011), and (3) tracking pollutant pathways and flow paths of polluted runoff. Accurate estimation of pollution load is imperative to assess the gap between target water quality standard and the field concentrations of pollutants. The reliable identification of CSAs facilitates effective watershed management by implementing proper practices in the most critical areas. The flow paths and travel time of polluted runoff impact the sediment and nutrient loads that reach receiving water bodies given that forests, grasslands, and wetlands retain pollutants by sedimentation, adsorption, and biotransformation (Chescheir et al., 1991; Uusi-Kamppa et al., 2000). The effective placement and design of pollutant control facilities such as buffer strips and artificial wetlands relies on detailed information about the pathways of pollutants from their points of origin to the discharge areas (Loáiciga et al., 2015; Sadeghi et al., 2017). However, the available tools including NPS pollution indices and models present significant challenges to provide all the three types of information cited above, especially the flow pathways and their impact on pollutant transfer.

NPS pollution indices, such as the Phosphorus Index (PI), are widely used to identify CSAs. Originally, the PI (Lemunyon and Gilbert, 1993) was designed for field-scale pollution risk ranking based on both "source" and "transport" characteristics. Subsequently, the PI was modified for watershed-scale assessment by improving the weighting method of hydrologic connectivity to a stream network (Gburek et al., 2000). More recently, a phosphorus index based on runoff travel time was developed to further improve the PI's capability to represent the effect of a drainage network on phosphorus loss potential (Buchanan et al., 2013). Improved PI methods combine empirical observations about source characteristics and knowledge about transport potential and are used for watershed-scale identification of phosphorus CSAs. The PI, however, is limited in its ability to simulate phosphorous dynamics given that it is primarily a tool for relative pollution risk assessment rather than for the quantitative estimation of pollution export.

Another approach to NPS pollution management is through the use of models. Empirical or "black-box" models, such as the Export Coefficient Model (ECM), have been successfully applied to the estimation of pollution loads from the small watershed scale to the regional and national scales (Johnes, 1996; Malve et al., 2012; Winter and Duthie, 2000). The classical ECM is a lumped model and only the spatial variation of land covers is accounted, which is not detailed enough for CSAs identification. By contrast, physically-based process models, such as Soil and Water Assessment Tool, or SWAT (Arnold et al., 1998), Hydrological Predictions for the Environment or HYPE (Lindström et al., 2010), and Annualized Agricultural Non-Point Source Pollution Model or AnnAGNPS (Bingner and Theurer, 2001), account for the spatial variations of soils, land use, topography and management practices. They simulate pollutant loads after calibration and can identify CSAs. However, these models are seldom used in practice by conservation specialists for delineating CSAs and for implementing measures to control pollutants emanating from non-point sources. The relatively infrequent application of the latter models might be explained by their generation of simulation results that are meaningful for naturally occurring hydrologic catchments within the landscape (usually subwatershed), while management of non-point pollutants in rural settings is meaningful at the farm-scale (Ghebremichael et al., 2013), which represents a human-induced partition of the landscape. Also, the farm-scale flow paths and travel times of runoff are not delineated by these models, and their impact on nutrient dynamics during transport is not accounted for. Another reason for the limited applications for the cited physically-based process models may be found in their complexity, which means that the data requirements, parameterization, and calibration make their application computationally and logistically burdensome, especially in large watersheds of regional scales (Alexander et al., 2002; Heathwaite, 2003).

This paper develops a Spatially and Temporally distributed Empirical Model for Phosphorus management (STEM-P) to address the limitations of the available tools in supporting accurate and cost-effective management. The STEM-P model satisfies three objectives: (1) reasonably accurate estimation of phosphorus export, (2) field or sub-field identification of CSAs, and (3) delineates the flow paths and considers travel time of phosphorus runoff. The STEM-P considers the impacts of flow pathways on phosphorus dynamics during transport. In addition, it is a process-based empirical model, that is, it relies on simple empirical equations and limited parameters to represent the most critical landscape processes (mobilization and delivery) that impact phosphorus loss for practical applications of pollutant control measures.

2. Method

2.1. Model development

Operational models for non-point source phosphorus management, such as Phosphorus Indicators Tools (Heathwaite et al., 2003) divide the processes by which phosphorus moves from the landscape to water bodies into three categories: storage, mobilization, and delivery. Storage is the balanced process of background phosphorus content that results from phosphorus input and output (e.g. harvest) in the landscape when precipitation does not occur. Mobilization is the process by which phosphorus moves from the landscape to the water pathways in soluble and particulate forms. The delivery process consists of the changes of phosphorous quantity and forms in surface runoff as it moves downstream overland or through the drainage network. It includes sedimentation, adsorption, plant uptake, microbial transformation, and other processes, resulting in the reduction of phosphorus content in pollutant runoff. STEM-P focuses on (i) the mobilization process by which phosphorus is released from a landscape to surface runoff, and on (ii) the delivery process of phosphorus as it moves with surface runoff. The mobilization process of phosphorous from non-point sources is assumed to be a zero-order mobilization mechanism. Its delivery is represented as first-order retention. The proposed STEM-P

model steps are portrayed in Fig. 1. The spatial resolution of STEM-P is a user-defined grid cell and the temporal step is daily.

2.1.1. Phosphorus storage

Phosphorus storage is a balanced process of the background content altered by phosphorus input and output. The balanced stored phosphorus during a specific period (P_{stored}) is calculated as follows:

$$P_{stored} = P_{background} + P_{surplus}$$
$$P_{surplus} = P_{input} - P_{output} \quad (1)$$

where $P_{background}$ is the background phosphorus content; $P_{surplus}$ is the surplus phosphorus, which is the difference between input phosphorus (P_{input}) and output phosphorus (P_{output}). Input phosphorus includes chemical and organic fertilizers, human and livestock wastes, and output phosphorus usually refers to phosphorus content in harvested crops from agricultural lands and may also be phosphorus removal by waste treatment facilities on residential and industrial lands.

2.1.2. Phosphorus mobilization

Non-point source phosphorus pollution is mainly mobilized by surface runoff. Field observation of surface runoff at the temporal scale of minutes or hours indicates that the phosphorus concentration varies with time. However, on an event basis or a daily time step, pollutant concentration in runoff is assumed to be constant, such as the Event Mean Concentration (EMC) used in water quality models (Lin, 2004; Liu et al., 2015). STEM-P assumes that the rate of phosphorus mobilization within a specific land cover is constant through days, since it is basically determined by the long-term storage process on soil surface. The mobilized phosphorus with surface runoff from landscape grid cell i ($P_{mobilized,I}$, in mg) is calculated as follow:

$$P_{mobilized,i} = m_i \cdot m_{adj} \cdot Q_i \cdot A_0 \quad (2)$$

where m_i is the zero-order mobilization rate of grid cell i, in $mg \cdot L^{-1}$; m_{adj} is the adjustment coefficient for the mobilization rate m; Q_i is the surface runoff depth in a simulation day on grid cell i, in mm; A_0 is the area of the grid cell of the model, in m^2.

The zero-order mobilization rate represents the risk of phosphorus mobilized by surface runoff from the landscape under a long-term storage balance. Since phosphorus input and output vary with land covers, the mobilization rate also varies with land covers. The best way to determine the mobilization rate is by long-term measurement of runoff phosphorus for different land cover types within the study area. The runoff should be collected from a land parcel having a similar size to that of the grid cell of simulation to reduce the scale effect. However, this on-site observation is time-consuming and has a high-level requirement of labor and facility resources, which would limit the model application. A method linking the mobilization rate (m) to stored phosphorus (P_{stored}) is herein proposed to reduce the number of land cover types that require on-site observation or to avoid on-site observation by applying literature values from climatologically similar regions.

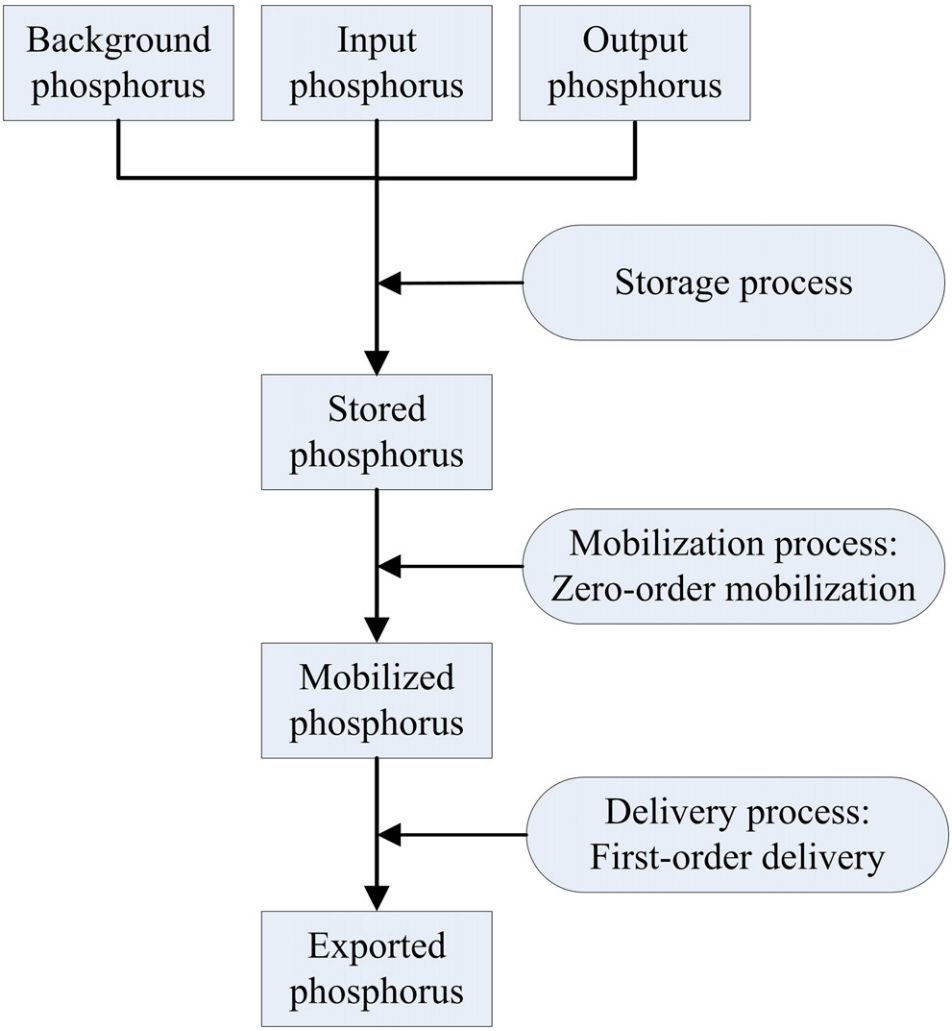

Fig. 1. The STEM-P model steps.

Common watershed models (such as SWAT, AnnAGNPS) usually use or modify the soil phosphorus (P) routines in Erosion Production Impact Calculator (EPIC) model, classify soil P into fresh organic P, humic organic P (including active and stable organic P), labile or solution inorganic P, active inorganic P, and stable inorganic P (Radcliffe and Cabrera, 2006). The P transferred by surface runoff is mainly labile P and active P. Fertilizers, human, and livestock waste are mainly in labile and active forms. Therefore, surplus phosphorus ($P_{surplus}$) is more likely to be mobilized by surface runoff than background phosphorus ($P_{background}$). STEM-P links the mobilization rate in land type k (m_k) to $P_{surplus}$ and $P_{background}$ with linear relations as follows:

$$m_k = k_1 \cdot P_{\text{surplus},k} + k_2 \cdot P_{\text{background}} \quad (3)$$

where k_1 and k_2 are the linear coefficients for $P_{surplus}$ and $P_{background}$ respectively. The mobilization rate on land types with no surplus phosphorus (such as forest and grassland without grazing) is $m_0 = k_2 \cdot P_{\text{background}}$. The background phosphorus within a study watershed is considered to be homogeneous, so that eq. (3) can be written as eq. (4):

$$m_k = m_0 + k_1 \cdot P_{\text{surplus},k} \quad (4)$$

Eq. (4) implies that the number of land cover types that require on-site observation can be reduced to only two: one type without surplus phosphorus, such as forest, to obtain m_0 value, and the other type with some surplus phosphorus to obtain m_k. Then, parameter k_1 is solved to calculate the m_k in other land types. If on-site observation in the study area is difficult to implement, then the two values (m_0 and m_k) can be obtained from the literature applicable to areas that are climatologically similar to the study region. In this case, the input and output phosphorus of the land type where the reference m_k value is obtained should be collected to estimate $P_{surplus,k}$ in eq. (4). The best reference values are from literatures conducting experimental research of field-scale runoff phosphorus concentrations. They can also be EMC values from the literature, since EMCs have similar meanings for the mobilization rates herein employed. Lin (2004) summarized published EMCs for different regions in the United States. The m_0 and m_k values from on-site observation may be not representative of the general characteristics of the study area, or there may be some scaling effects; and the values obtained from the reference regions may be not the same as those of the study area. Considering this uncertainty, an adjustment coefficient for mobilization rate (m_{adj}) is incorporated in Eq. (2) to adjust the absolute values of m_k while maintaining the relativity of m_k values among land cover types.

2.1.3. Phosphorus delivery

Physical, chemical, and biological retention of phosphorus over vegetated buffers, in wetlands, reservoirs, and streams has been documented (Hesse et al., 2013; Roberts et al., 2012; Uusi-Kamppa et al., 2000). In spite of the complexity of the delivery process, less complex approaches maybe reasonably adequate to model water quality. This is so because only minor improvements in the accuracy of simulations might be achieved with models of high complexity, as documented by Hesse et al. (2013). The phosphorous delivery process is represented as a first-order retention mechanism in STEM-P:

$$P_{\text{export},i} = P_{\text{mobilized},i} \cdot \exp\left[\sum_j \left(-\delta_j \cdot \delta_{\text{adj}} \cdot T_j\right)\right] \quad (5)$$

where $P_{export,i}$ is the part of phosphorus mass mobilized from grid cell i that enters a target water body as a result of the delivery process, in mg; δj is the first-order delivery rate of grid cell j along the flow path of surface runoff generated from grid cell i, d^{-1}; Tj is the travel time of phosphorus runoff across grid cell j, in d; δ_{adj} is the adjustment coefficient for delivery rate δ_j. The delivery process as a first-order retention mechanism has been observed in field studies and is used in practical modeling. Chescheir et al. (1991) found phosphorus removal in a forested wetland to be well described by the first order decay model in a two-year field study. The SPARROW model used first-order dynamic to simulate phosphorus transformation in streams and in reservoirs for large-scale modeling (Smith et al., 1997).

The first-order delivery rate (δ_j) varies with land cover types. Previous phosphorus removal research suggests that wetlands are more effective in retaining total phosphorous (TP) than ponds, possibly due to shallower depth, and dense vegetation (Uusi-Kamppa et al., 2000). The impacts of vegetation types (trees or grass) are not significant in vegetated buffers (Duchemin and Hogue, 2009; Syversen, 2005). SPARROW applied in the USA demonstrated a larger decay rate of total phosphorous (TP) in reservoirs than in streams because of differences in settling rates of sediment-bound phosphorus (Smith et al., 1997). To summarize, the retention rate generally increases with increasing vegetation density, and decreases with increasing flow velocity and flow depth. Thus, the δ_j value is largest for forest and grassland, followed in decreasing order by wetland, lakes, reservoirs, and streams. Agricultural land and residential areas are generally regarded as sources of phosphorus; yet, there is some level of physical retention due to sedimentation. Field research on these lands is limited. Thus, the δ_j values of these lands is herein determined by comparing with other better-known land covers. Table 1 lists the STEM-P recommended values for the delivery coefficients of different land cover types. The recommended values would be adjusted according to the land characteristics of the study area, such as vegetation cover density, surface roughness, the water depth of lakes or ponds, etc. An adjustment coefficient for delivery rate (δ_{adj}) in a manner akin to the adjustment coefficient for mobilization rate is herein introduced to account for the differences between our reference values shown in Table 1 and the conditions of the study areas.

2.1.4. Phosphorus transfer in baseflow

STEM-P applies the mobilization and delivery equations described above to simulate the mobilized phosphorus and exported phosphorus from each landscape grid cell to the target water body with surface runoff on a daily scale. Phosphorus transferred with baseflow is also simulated in STEM-P with the following equations:

$$\begin{aligned} P_{\text{gw}} &= \text{PCONC}_{\text{gw}} \cdot O_{\text{b}} \cdot 24 \cdot 3600/1000 \\ P_{\text{rf}} &= \text{PCONC}_{\text{rf}} \cdot O_{\text{rf}} \cdot 24 \cdot 3600/1000 \end{aligned} \quad (6)$$

where P_{gw} and P_{rf} are the mass of phosphorus transferred with groundwater flow and lateral return flow respectively, in $kg \cdot d^{-1}$; O_b and O_{rf} are the groundwater flow and lateral subsurface flow that reach the target water body each day, in $m^3 \cdot s^{-1}$; $PCONC_{gw}$ and $PCONC_{rf}$ are the average P concentration in groundwater flow and lateral subsurface flow, respectively, in $mg \cdot L^{-1}$. These two parameters can be determined from long-term monitoring data or from data generated by the knowledge of local experts. If these are not available, they are determined by

Table 1
The STEM-P recommended values of the delivery rates for different land types.

Land cover type	Delivery rate $\delta(d^{-1})$	Reference
Forest/grassland	0.50	Chescheir et al. (1991)
Wetland[a]	0.40	
Orchard	0.35	
Lake/reservoir/pond	0.30	Smith et al. (1997)
Agricultural field[b]	0.25	
Stream	0.20	Smith et al. (1997)
Residential land	0.10	

[a] Wetland refers to land with less than or normal density of vegetative cover, otherwise the delivery rate of forested wetland is recommended to be the same as that of forest/grassland.
[b] Agricultural field refers to dry field and paddy field during the period when the surface is not flooded.

calibration. The calibrated value of $PCONC_{gw}$ should be less than that of $PCONC_{rf}$ given that phosphorus concentration usually decreases with increasing soil depth.

2.1.5. Special characteristics of phosphorus transfer in paddy fields

Paddy fields have special characteristics concerning phosphorus transfer during the flooding period. The phosphorus mobilization process does not result from interaction between runoff and soil surface in flooded paddy fields as it does in other land types. Rather it is controlled by the direct release of the flooded water. Therefore, a separate parameter, the average P concentration of flooded water ($PCONC_{pddy}$, in $mg \cdot L^{-1}$) is used to simulate mobilized phosphorus for flooded paddy field, instead of the mobilization rate *m*. Previous research has established that the P concentration of flooded water greatly increases on the day of fertilizer application. This is followed by an exponentially decline afterward and levels off about 12 days later to a concentration value similar to that prevailing before fertilizer application (Shi et al., 2013). Farmers usually avoid applying fertilizers in paddy fields during rainy days. For this reason STEM-P assumes the $PCONC_{pddy}$ is constant during simulations for the flooded period. $PCONC_{pddy}$ can be obtained by long-term field observation, or by model calibration.

The delivery process from flooded paddy fields is negligible because the average P concentration of flooded water is used instead of the mobilization rate. Hence, the delivery rate of flooded paddy fields is set to be zero in STEM-P.

The soil of flooded paddy field is saturated, which promotes phosphorus desorption and leaching. Previous research has demonstrated that in wheat-rice rotation fields the phosphorus leaching during the rice season is dramatically greater than that during the wheat season (Li et al., 2009). Therefore, phosphorus transfer with groundwater flow simulated by STEM-P differentiates between its sources, either from flooded paddy fields or from other lands. In a watershed with areas covered with paddy fields there are two phosphorous concentrations used by STEM-P, namely, the average P concentration of groundwater in land devoid of paddy fields ($PCONC_{gw}$), and the average P concentration in groundwater flow from flooded paddy field ($PCONC_{gw\_pddy}$). STEM-P applies these two concentrations to simulate P transfer with groundwater flow.

The parameters $PCONC_{pddy}$ and $PCONC_{gw\_pddy}$ are determined from monitoring data if long-term observation of the phosphorus concentration in flooded water and leaching water from paddy fields are available. If not, they are determined by calibration, and the default value of $PCONC_{gw\_pddy}$ is half of the average P concentration of flooded water ($PCONC_{pddy}$).

2.1.6. Hydrologic basis of STEM-P

STEM-P is a spatially and temporally distributed non-point source pollution model. Its model inputs include: distributed daily surface runoff depth and travel time of surface runoff on a grid-cell basis, time series of daily surface flow, groundwater flow and lateral return flow at the receiving water body. Daily groundwater flow should be recorded separately for flooded paddy field and for other lands whenever paddy fields exist in a watershed. The above spatial and temporal hydrologic information can be provided by distributed hydrologic models. Theoretically, any distributed hydrologic model that provides this information can be input to STEM-P. However, commonly used distributed hydrologic models seldom report the travel time of surface runoff across the landscape on a grid-cell basis, probably because in-stream hydrographs are their goals. Hence, this study applies the Distributed Hydrologic Model for Watershed Management developed previously (DHM-WM, Li et al., 2017a; Li et al., 2017b). DHM-WM delineates the flow path of surface runoff and calculates the travel time on a grid-cell basis (Li et al., 2017a), which allows the consideration of the travel time in the simulation of the delivery process by STEM-P. In addition, a recent version of DHM-WM simulates reasonable surface runoff (as a depth) in generation areas based on distributed representation of soil moisture variation accounting for both local and global water balance, making it more suitable for watersheds featuring infiltration-excess and saturation-excess runoff generation mechanisms (Li et al., 2017b).

2.2. Model application in a Forest/agricultural watershed

2.2.1. Watershed description

The STEM-P model was applied to the Fengyu Watershed located on the headwater area of Erhai Lake, an alpine fault lake in Yunnan Province, China (see Fig. 2). The Fengyu Watershed covers an area of 217 km^2, and its altitude ranges from 2079 m to 3621 m. It features a subtropical highland monsoonal climate. The temperature variation within a year is minor, and snow seldom falls in Winter. There are well differentiated dry and wet seasons within a year, and most rainfall falls between June and October. The dominant activity of the area is agriculture. Phosphorous originates primarily from non-point sources: fertilizers, human and livestock waste, which facilitates the comparison of simulated phosphorus from STEM-P to observed data. Study watersheds featuring urbanized areas, phosphorus discharge from point sources (factories and wastewater treatment facilities) would add more complexity to the testing of the STEM-P results. The monitoring station is located at the watershed outlet, in the northeastern portion of the watershed. Precipitation, streamflow discharge, and phosphorus concentration were measured at the station daily.

2.2.2. Distributed data

The input data to STEM-P include digital elevation model (DEM) (Fig. 2), distributed maps of land cover, surface runoff depth and travel time of surface runoff. Fig. 3 is exemplary of the latter three data, which also depicts the map of soil type distribution. The size of grid cells of these distributed data is 25 m, which is the resolution of DEM data. The DEM resolution determines the accuracy of flow pathway analysis and the scale of landscape processes impacted by flow pathways. It can be inferred from Fig. 3(a) that 51.6% of the watershed is covered by forest, followed with 18.2% by grassland, 15.2% by paddy fields, 9.3% by dry fields, 3.4% by orchards, and 2.3% being residential, and it features three small lakes/reservoirs. Fig. 3(b) shows that there are 11 types of soils in the watershed. Among them, Brown laterite, Red limestone and Funi have a very high content of clay and very low water transmissivity. By contrast, Mahuitang, Maheitang, Maheihui, and submergenic paddy soil have a very high content of sand and high water transmissivity. Fig. 3(c) and (d) are examples of distributed surface runoff depth and travel time calculated for July 23, 2013, by DHM-WM. The hydrologic results were previously calibrated with observed streamflow data at the watershed outlet in 2012 and validated in 2013, with an annual percent bias less than 15%, daily coefficient of determination greater than 0.70, and reasonable baseflow percentage between simulated and observed values for both years. The highland region of the watershed generally did not generate surface runoff (see Fig. 3(c)) because of the runoff generation mechanism governing this region and the water use for paddy fields. The highland region is covered mainly by forests and grasslands, and is underlain by sandy, well drained soils where infiltration-excess runoff is seldom generated. Also, this region is not easily saturated because irrigation for paddy fields lowers the subsurface water table in the rainy seasons. Hence, saturation-excess runoff only occurred during very wet days along riparian areas and gullies where subsurface soil water concentrated. The distributed data ensure that mobilized phosphorus and exported phosphorus are simulated on a grid-cell basis in STEM-P.

2.2.3. Determination of the mobilization rate

The input phosphorus, output phosphorus, surplus phosphorus data were collected for each land cover type, and the mobilization rate is calculated with Eq. (4) with two reference values from a climatologically similar region (See Table 2). The input phosphorus for agricultural lands (paddy fields, dry fields, and orchards) was calculated by statistics

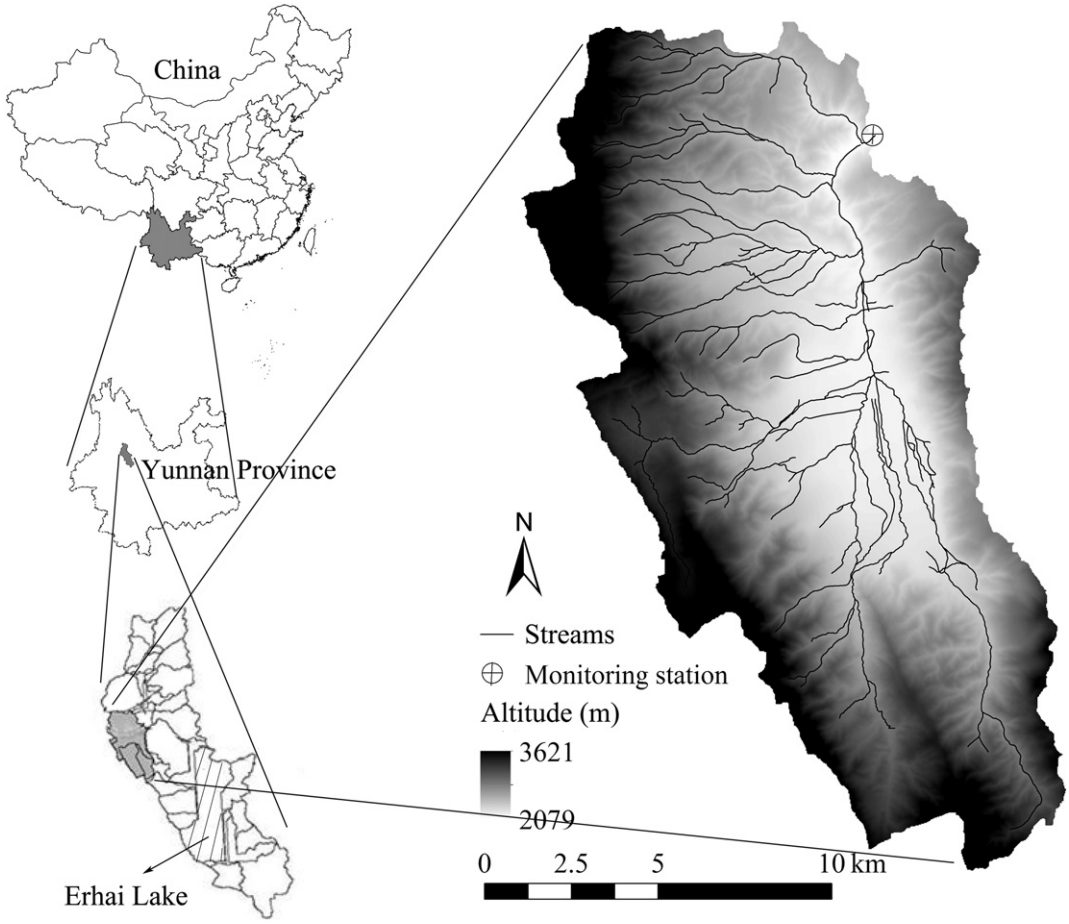

Fig. 2. The location and geographic features of Fengyu Watershed.

of fertilizer and manure application in the study area. Paddy fields are typically cultivated with rice-broad bean rotation within a year, and dry fields are typically cultivated with corn-broad bean rotation within a year. Their phosphorus input is the sum of fertilizer and manure applied for both cultivation seasons in a year. The non-hydrologic output of phosphorus from the agricultural lands is the mass of phosphorus contained in the harvested crops. In residential areas, the input phosphorus equals the sum of human waste and livestock waste. The non-hydrologic output of phosphorus is the amount of livestock waste that was collected to be used as manure elsewhere. Phosphorus removal in residential areas was assumed to be negligible given that there is rarely public sewage and waste treatment facilities in the study region. The reference mobilization rates are from on-site observations conducted in 1991 in the nearby Dianchi watershed (Gu et al., 1991). There has been a substantial increase in fertilizer and manure inputs, and in crop harvest since then (statistics in Table 2), which was accounted by Eq. (4) in calculating the mobilization rates of other land covers in the case study.

2.2.4. STEM-P calibration and evaluation of model performance

Phosphorus concentration at the watershed outlet was observed from 2012 to 2013. The water samples were collected from the stream daily. Their total phosphorus concentrations were measured with the ammonium molybdate spectrophotometric method after digestion in the laboratory. The model was calibrated with data from 2012 by comparing daily observed phosphorus concentrations with simulated values by STEM-P. The calibrated set of parameters was determined by optimizing the closeness of match of the visual graphs and several statistical indicators: the annual percent bias (P_{bias}), the daily and monthly coefficient of determination (R^2), and the Nash-Sutcliffe coefficient (E_{NS}). Model validation was conducted with data in 2013 using the same indicators of calibration. Other indicators, such as the root mean square error (RMSE) and Persistent Index (PI), can be used for model evaluation (Wu et al., 2010). This study chose P_{bias}, R^2 and E_{NS} because they are the most commonly used in evaluating water quality models, and general criteria for model performance have been summarized by reviewing a number of publications (Moriasi et al., 2015) as follows: If P_{bias} is less than $\pm$30%, monthly R^2 is greater than 0.40, and monthly E_{NS} is greater than 0.35, the model performance is herein deemed satisfactory; if P_{bias} is less than $\pm$20%, monthly R^2 is greater than 0.65, and monthly E_{NS} is greater than 0.50, the model performance is herein considered as good.

2.2.5. Analysis of critical source areas

The critical source areas within the Fengyu Waterhsed were selected based on the distributed annual exported phosphorus with surface runoff during 2012–2013 simulated by STEM-P. The areas with average annual exported phosphorus exceeding the watershed mean value by more than two times the standard deviation were classified as extremely critical source areas (CSAs A). The areas with annual exported phosphorus exceeding the watershed mean by more than one standard deviation but less than two times the standard deviation were classified as critical source areas (CSAs B).

3. Results

3.1. Calibrated parameters

The STEM-P has at most 6 calibration parameters, which is the case in Fengyu Watershed, where a large area of paddy fields exists, and

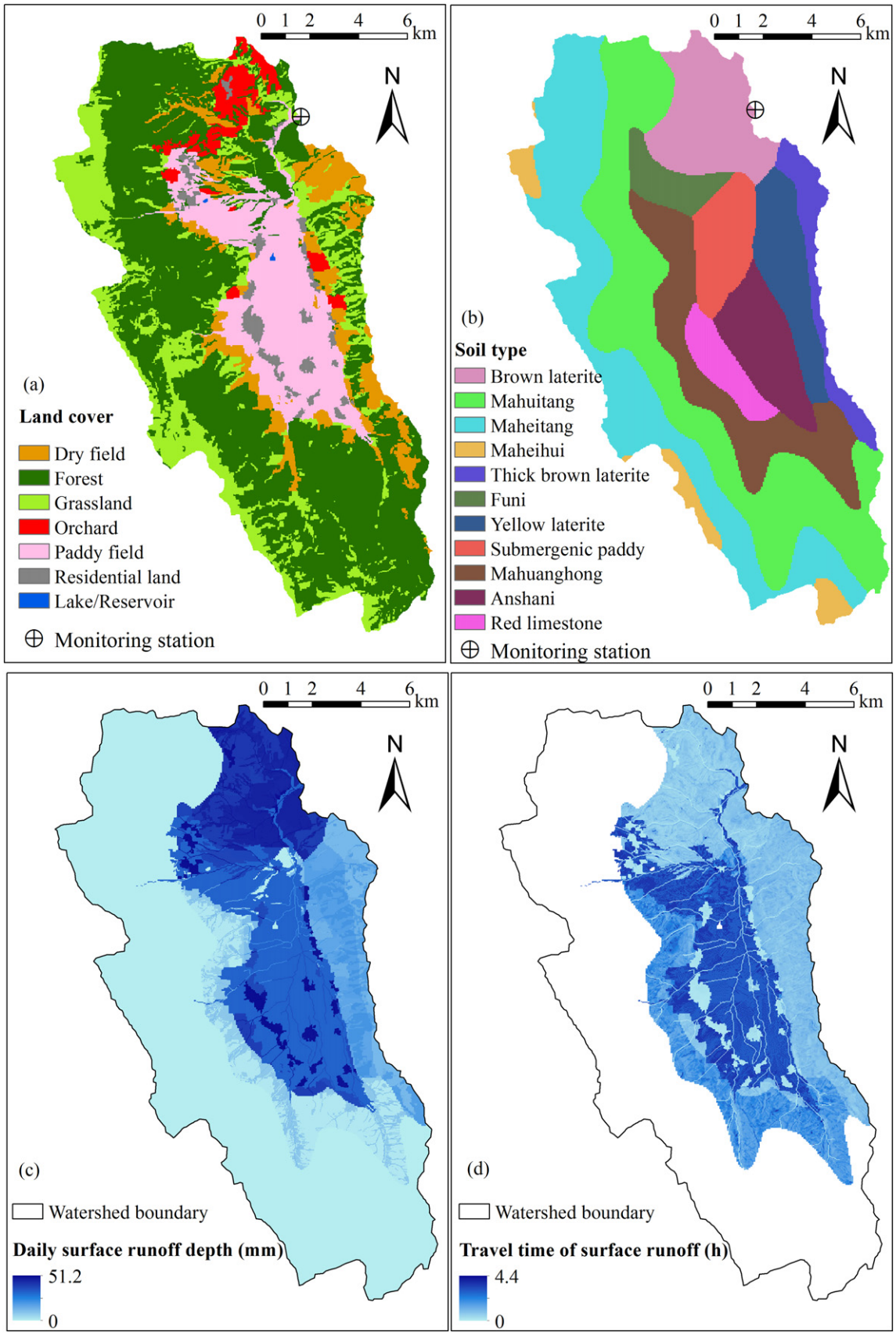

Fig. 3. Examples of distributed data for the Fengyu Watershed; (c) and (d) are simulated values from a hydrologic model (DHM-WM) for July 23, 2013.

Table 2
Mobilization rate determined for the Fengyu Watershed with statistics about surplus phosphorus.

Land cover	m ($mg \cdot L^{-1}$)	Input phosphorus ($kg \cdot ha^{-1} \cdot yr^{-1}$)	Output phosphorus ($kg \cdot ha^{-1} \cdot yr^{-1}$)	Surplus phosphorus ($kg \cdot ha^{-1} \cdot yr^{-1}$)
Paddy fields[a]	1.466	187	98	89
Dry fields	1.553	197	97	100
Forest	0.765	Negligible	Negligible	0
Grassland	0.765	Negligible	Negligible	0
Orchard	1.631	148	38	110
Residential land	1.642	313	202	203
Reference forest[b]	0.765	Negligible	Negligible	0
Reference field[b]	0.980	38	11	27

[a] The mobilization rate for paddy fields is used for unflooded period only. During flooded period use the average phosphorus coefficient of flooded water ($PCONC_{pddy}$) instead.
[b] The mobilization rates of reference forest and agricultural fields are from on-site observations in Dianchi watershed, a climatologically similar area near the study area.

long-term observations of flooded water and leaching water on paddy field are unavailable. The calibrated parameters are listed in Table 3. The calibrated adjustment coefficient for mobilization rate (m_{adj}) was 0.60, smaller than 1.0, which meant the calibrated mobilization rates were less than the values listed in Table 2. One probable reason for this finding is that the background phosphorus content in Fengyu Watershed is lower than that of the reference Dianchi watershed. The Dianchi watershed is reported as a region with relatively high background phosphorus content (He, 2015). Another reason may be that the statistical value of output phosphorus was underestimated in the Fengyu watershed, because part of the agricultural residue was removed from the field for the purpose of feeding livestock, such as cattle. Livestock is raised by individual farmers and the actual amount of crop residue used as feed is difficult to estimate. For this reason, this component of phosphorus was not included in the output phosphorus in Table 2. The calibrated adjustment coefficient for delivery rate (δ_{adj}) was 1.20, larger than 1.0, which meant the calibrated delivery rates were greater than the recommended values in Table 1. The probable reasons for this finding include: the vegetation density in Fengyu watershed is greater than that in the reference areas obtained from the literature; the temperature and humid condition in the subtropical Fengyu watershed improves the activity of microorganism and biotransformation rate. The calibrated value of $PCONC_{gw}$ was 0.065 $mg \cdot L^{-1}$, which is reasonable given its similarity to the average value (0.072 $mg \cdot L^{-1}$) of observed phosphorus concentration in streamflow on no-rain days during the broad bean season. The calibrated value of $PCONC_{rf}$ was 0.078 $mg \cdot L^{-1}$, slightly larger than the calibrated $PCONC_{gw}$ as expected, since phosphorus concentration is usually larger in the soil profile than that water in groundwater. The $PCONC_{pddy}$, a paddy-field specific parameter, was calibrated to be 0.750 $mg \cdot L^{-1}$, which about the same as the observed phosphorus concentration of flooded water in paddy fields 12 days after fertilizer application, reported in a field experiment research conducted in the same region (Shi et al., 2013). The calibrated $PCONC_{pddy}$ value was smaller than the adjusted mobilization rate of dry fields (0.932 $mg \cdot L^{-1}$), which is the multiple of the mobilization rate for dry fields (1.553 $mg \cdot L^{-1}$) and the calibrated m_{adj} parameter (0.60). This is also reasonable estimate since surface runoff on dry fields generally has larger turbulence and mobilizes more particulate phosphorus than in paddy fields. The calibrated $PCONC_{gw\_pddy}$ value was 0.375 $mg \cdot L^{-1}$, which equaled the default value, i.e., half of the calibrated $PCONC_{pddy}$ value.

Table 3
Calibrated parameters of STEM-P in the Fengyu Watershed.

Parameters	Description	Calibrated value
m_{adj}	The adjustment coefficient for mobilization rate	0.60
δ_{adj}	The adjustment coefficient for delivery rate	1.20
$PCONC_{gw}$	The average P concentration of groundwater flow from lands other than flooded paddy fields ($mg \cdot L^{-1}$)	0.065
$PCONC_{rf}$	The average P concentration of lateral return flow ($mg \cdot L^{-1}$)	0.078
$PCONC_{pddy}$	The average P concentration of flooded water in flooded paddy fields ($mg \cdot L^{-1}$)	0.750
$PCONC_{gw\_pddy}$	The average P concentration of groundwater flow from flooded paddy fields ($mg \cdot L^{-1}$)	0.375

3.2. Model performance

The daily total phosphorus (TP) concentration at the watershed outlet was calculated by dividing the STEM-P simulated daily exported phosphorus mass by the DHM-WM simulated daily streamflow. The time series of simulated daily TP concentrations during 2012–2013 were compared with the daily observed TP concentrations (Fig. 4). Apparent underestimation was detected from August 6 through August 18 of 2012. This is mainly due to the rise of phosphorus concentration from 0.15 $mg \cdot L^{-1}$ on August 5 to 3.92 $mg \cdot L^{-1}$ on August 6 caused by a debris flow event, which occurred only once during the last three decades according to local residents. The associated degradation of in-channel water quality had a long-lasting effect and the phosphorus concentration did not fall below 1.1 $mg \cdot L^{-1}$ until August 19. The precipitation on August 6 was 33 mm (Fig. 4), a normal value during the study period, which indicated the debris flow was not caused by extreme precipitation event, but by other yet-to-be determined reasons. This kind of unusual events are not incorporated in standard simulation models. For this reason, and to facilitate model evaluation, the period from August 6 to August 18 was excluded from further model evaluation.

Fig. 4 shows that the trends of simulated TP concentration generally matched with the observed data except for a few discrepancies. The simulated TP concentration generally varied synchronously with precipitation events, rising on rainy days and declining thereafter. However, the observed TP concentration also rose on several no-rain days, such as May of 2012, the early January of 2013, October 16 and November 19 in 2013. This was probably caused by artificial discharge of residential wastewater, because there are not industrial dischargers within the study watershed and other non-point sources of phosphorus are driven by rainfall events. Besides this kind of discrepancy, an underestimation of phosphorus concentration was also detected in August and early part of September in 2013. August of 2013 was a period when rainfall quantity was relatively low in the wet season and evapotranspiration was relatively high, which increased phosphorus concentration of flooded water on paddy fields. However, the $PCONC_{pddy}$ parameter was constant over time in the current STEM-P, which may explain the underestimation.

The statistics of model performance during 2012–2013 are shown in Table 4. According to the evaluation criteria (Moriasi et al., 2015), STEM-P's performance is good for the calibration and validation periods. The underestimation in August and early September of 2013 detected in Fig. 4 caused the higher P_{bias} and lower monthly R^2 and E_{NS} in 2013 than that in 2012. Compared to monthly R^2 and E_{NS}, the daily R^2 and E_{NS} are relatively low. The rise of phosphorus concentration without rainfall flush is one reason, and the constant $PCONC_{pddy}$ parameter used in STEM-P is likely the other reason.

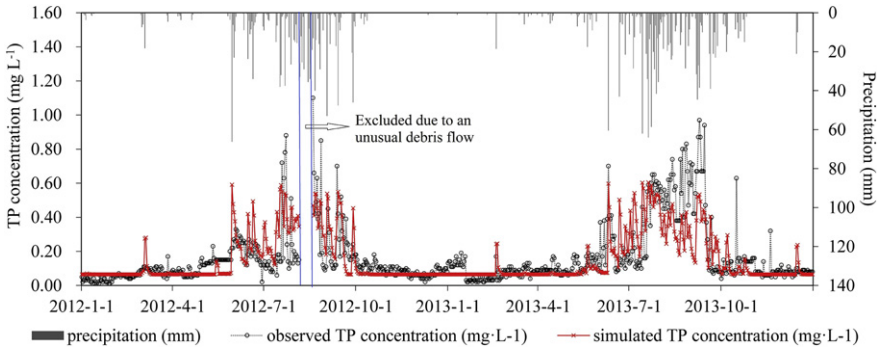

Fig. 4. Comparison of daily observed total phosphorus (TP) concentration and simulated TP concentration at the watershed outlet.

3.3. Spatial and temporal distribution of mobilized and exported phosphorus

The mobilized and exported phosphorus simulated by STEM-P in the Fengyu Watershed have uneven spatial and temporal distributions. Fig. 5 depicts the spatial distributions of mobilized and exported phosphorus on three typical rainy days. Fig. 5(a) and (b) are the simulated results on June 10, 2013, when there was rainfall of 60.5 mm. This day was on the early part of wet season and the watershed was relatively dry, with an average relative soil moisture content of 0.38 simulated by DHM-WM. As can be seen in Fig. 5(a), the spatial distribution of mobilized phosphorus was related to the spatial distribution of soils and land covers (shown in Fig. 3). There was no mobilized phosphorus on paddy fields since no surface runoff was simulated by DHM-WM. The large values of mobilized phosphorus occurred mainly on residential areas, orchards and dry fields. In addition, on the same land cover type, mobilized phosphorus varied with soil types. Mobilized phosphorus was extremely high on brown laterite and red limestone soils, since these two soils are likely to generate surface runoff. Besides soils and land covers, the exported phosphorus (Fig. 5(b)) was also impacted by topographic locations. The grid cells with similar mobilized phosphorus had different exported phosphorus after the delivery process due to their different flow routes. For instance, the exported phosphorus from land parcels A, B and C (marked in Fig. 5) were 0.90 $mg \cdot m^{-2}$, 2.8 $mg \cdot m^{-2}$, and 3.4 $mg \cdot m^{-2}$ respectively while their mobilized phosphorus were all about 5.2 $mg \cdot m^{-2}$. Runoff generated on land parcel A moved through some areas (forest on well-drained soil) that did not generate runoff, thus the flow velocity was reduced and phosphorus was greatly retained. By contrast, the flow paths of land parcels B and C all generated surface runoff. But the overland flow path of land parcel B was longer and included a higher percentage of forest than that of land parcel C, so that the exported phosphorus from land parcel B was less than that of land parcel C.

Fig. 5(c) and (d) show the simulated results for July 23, 2013. This day had a rainfall of 58.5 mm and was in the middle of the wet season. The watershed moisture condition was normal, with an average relative soil moisture of 0.58 simulated by DHM-WM. The sum of simulated exported phosphorus through the watershed was 1421 kg, greater than the 644 kg on June 10. This was mainly because more surface runoff generated on July 23 due to a wetter condition, which mobilized more phosphorus. The exported phosphorus simulated on July 23 was 1310 kg, also greater than the 566 kg on June 10. This indicates that the export ratio (the ratio of exported phosphorus to mobilized phosphorus) on July 23 (0.92) was also greater than that on June 10 (0.88). For one thing, the delivery rate of flooded paddy field was set equal to zero in STEM-P, which resulted in a high export ratio from paddy fields and increased the general export ratio on July 23. For another, the larger surface runoff generated on July 23 led to a higher flow velocity and shorter travel time, which also increased the export ratio. For instance, the forests on the flow path of land parcel A generated runoff on July 23, and the export ratio was 0.70, significantly greater than the 0.13 on June 10.

Fig. 5(e) and (f) depict the simulated results on September 20, 2013, with a rainfall of 39.0 mm. The watershed was already very wet, with an average relative soil moisture content of 0.77 simulated by DHM-WM. This day was about a week before rice harvest, so that the flooded water on paddy fields had already drained out. Therefore, unlike July 23, the surface runoff and related mobilized phosphorus on paddy fields distributed unevenly on September 20 due to soil transmissivity as well as topographic location. It is seen in Fig. 5(e) and (f) that the exported phosphorus was apparently reduced after delivery process compared to the mobilized phosphorus on most areas. In general, the mobilized phosphorus through the watershed was 586 kg and the exported phosphorus was 447 kg. So, the general export ratio was 0.76, which was the smallest among the three typical days.

According to Eq. (5) the phosphorus export ratio is theoretically related to the travel time of the surface runoff and the land types along flow paths. It is seen in Fig. 5 (e) and (f) that the export ratio is impacted by the length of the flow paths, the land types, and the runoff depth along flow paths. The land parcel D (marked in Fig. 5 (e), (f)) was an orchard, with a high mobilized phosphorus of 31.9 $mg \cdot m^{-2}$. But its exported phosphorus was reduced to 22.5 $mg \cdot m^{-2}$ due to a long overland flow path (1765 m) containing a small part of forest. By contrast, orchard land parcel E (marked in Fig. 5 (e), (f)), had a similar mobilized phosphorus but a much higher exported phosphorus (30.1 $mg \cdot m^{-2}$), because its overland flow path was only 332 m and was all through orchard. The runoff depth on flow paths is also a key factor influencing the export ratio. Although land parcel D had a longer overland flow path than land parcel B (1293 m) and C (1104 m), its export ratio (0.71) was larger than land parcel B (0.45) and C (0.59). This was mainly because the flow path of land parcel D was through Brown laterite and generated more runoff, while the flow paths of land parcels B and C was through Yellow laterite and generated less runoff. Therefore, the phosphorus export ratio decreases with longer flow paths, larger percentage of natural lands with high delivery rates along the flow paths, and less runoff generated along the flow paths.

Table 4
Statistics of STEM-P performance in simulating phosphorus concentration.

	P_{bias} (%)	Daily		Monthly	
		R^2	E_{NS}	R^2	E_{NS}
Calibration (2012)	−7.1	0.45	0.33	0.90	0.80
Validation (2013)	18.1	0.59	0.55	0.77	0.72

3.4. Identification and analysis of critical source areas

The simulated annual phosphorus export from Fengyu Watershed was 21,100 kg, 76% of which was transported by surface runoff. The spatial distribution of this part of the exported phosphorus was further analyzed, and critical source areas were identified (Fig. 6). Phosphorus loss

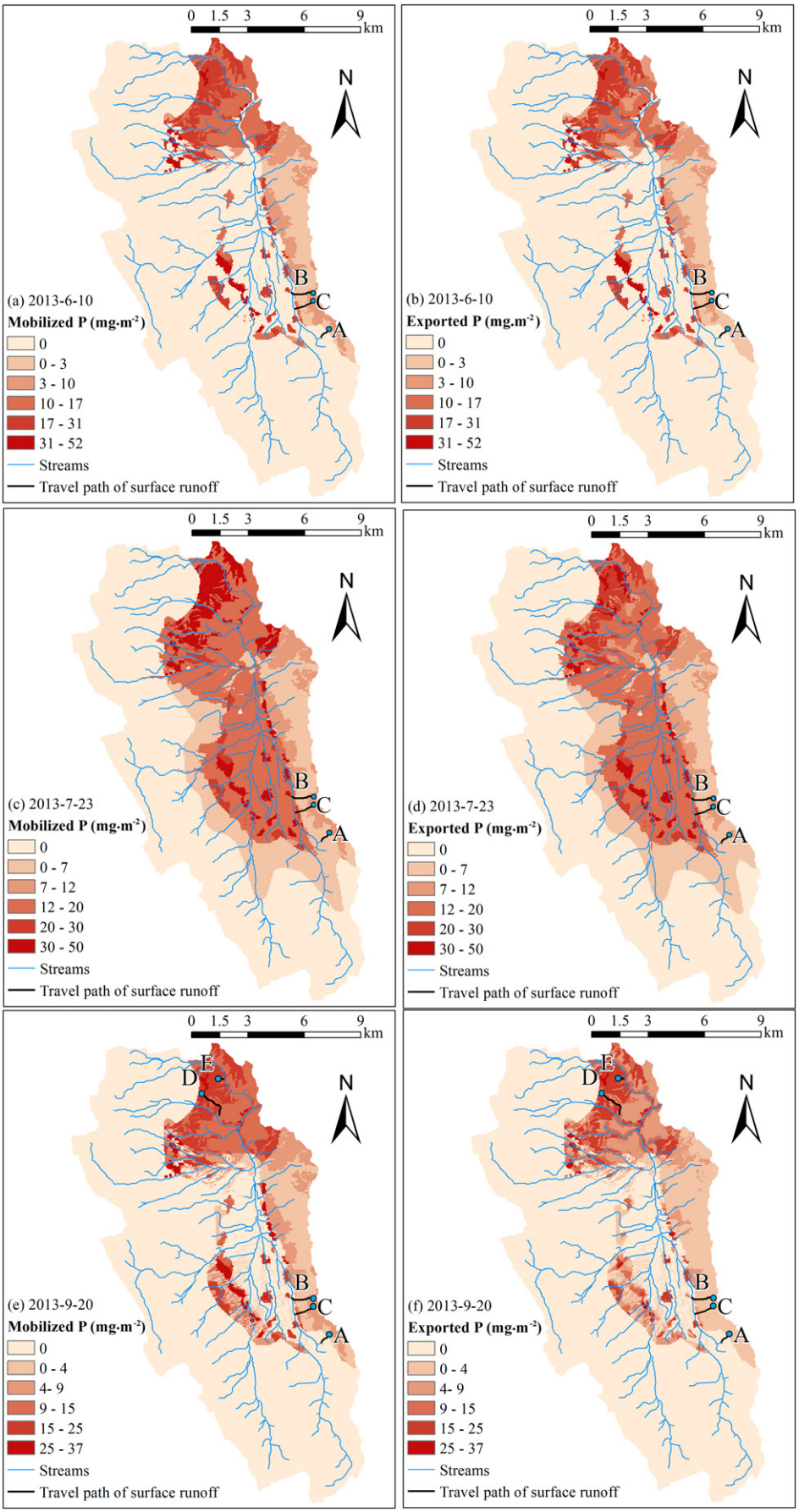

Fig. 5. Spatial distributions of mobilized and exported phosphorus simulated by STEM-P on typical rainy days in the Fengyu Watershed.

with surface runoff greatly varied across the watershed. Phosphorus export did not occur on 48.8% of the watershed, which is covered mainly by forests and grasslands and underlain by sandy, well-drained soils Maheihui, Maheitang and Mahuitang, where surface runoff is seldom generated as shown in Fig. 3(c). In fact, in this region there was only a small amount of phosphorus exported along riparian reaches and through gullies, where soil water concentrates and saturation-excess runoff is generated on some very wet days. In contrast, the middle and northeast areas of the Fengyu Watershed are at higher risk of phosphorus loss. The CSAs A covered only 3.4% of the watershed area, yet, it contributed 25.2% of the phosphorus export. The CSAs B covered 17.1% of the watershed area and accounted for 55.3% of the phosphorus export. These CSAs should be priorities of non-point source phosphorus control.

It is worthy of notice that a pronounced variation of TP export was detected within the same land cover. The square marked dry field shown in Fig. 6 is an instance. The differences between soils and geographic locations explain why the same land cover field can be a CSA A, a CSA B, or not critical source area of phosphorus loss. The STEM-P results are reported at a grid-cell resolution (25 m in the case study) and managers can resolve these sub-field variations of phosphorus loss risk advantageously for the purpose of watershed management under limited resources.

The hydrologic input data and the STEM-P simulations produced calculations of the annual surface runoff, average export ratio, annual exported phosphorus per unit area, and annual exported phosphorus (Table 5). These calculations allow further analysis of the reasons for the CSAs' high phosphorus loss risk. The CSAs A are extremely risky with a large amount of annual exported phosphorus per unit area (514.7 $kg \cdot km^{-2}$). This is mainly related to the large amount of surface runoff (586.4 mm), which provides large mobilization capacity. The CSAs A are composed of 51% residential areas, 27% orchards, 18% dry fields, and 4% paddy fields. Besides residential areas, they are all located on brown laterite soil that is likely to generate surface runoff. Residential areas also tend to generate surface runoff because part of their surface is impervious, and they generally lack vegetative cover. This explains why residential areas have the highest annual surface runoff

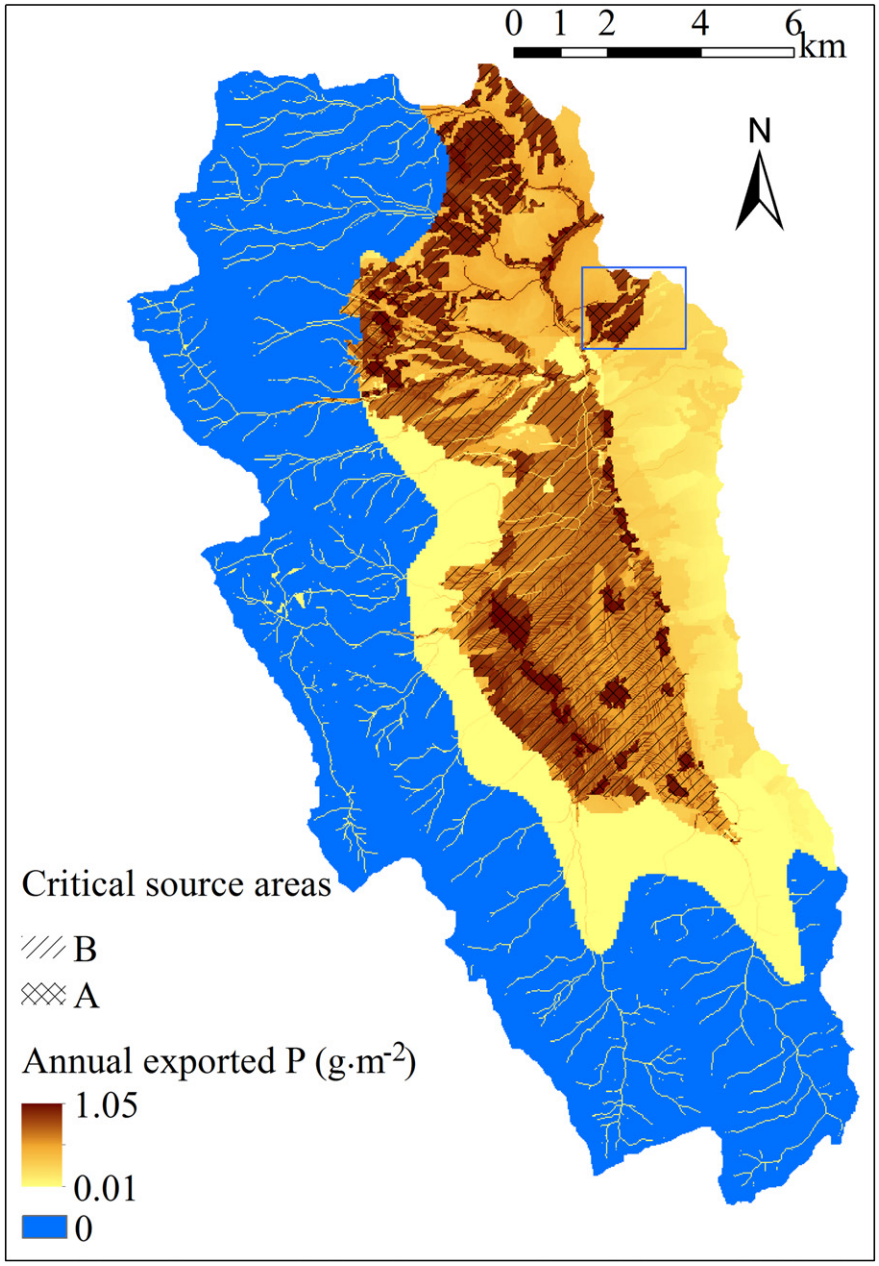

Fig. 6. Spatial distribution of annual exported phosphorus with surface runoff in the Fengyu Watershed simulated by STEM-P.

and exported phosphorus per unit area among the four land covers. By contrast, the export ratio from residential areas is the lowest among the four land covers. This is probably caused by their locations. These residential areas are generally further away from stream networks and/or have more forests/grassland on their flow paths than their counterpart orchards and dry fields. Therefore, it is recommended that pollution control for the residential areas in CSAs A focus on increasing on-site phosphorus removal by facilities such as biogas tanks, and reducing surface runoff by converting impervious surface into semi-impervious, and placing stormwater control measures such as rain barrels. Unlike residential areas, the agricultural lands (orchards, dry fields and paddy fields) in CSAs A exhibit large surface runoff as well as large export ratio. Thus, pollution control for these lands must account for the processes of storage, mobilization, and delivery.

The average annual exported phosphorus per unit area of CSAs B is 243.1 $kg \cdot km^{-2}$, much less than that of CSAs A, but still risky. Their annual surface runoff (331.2 mm) is less than that of CSAs A; while their average export ratio (0.91) is larger than that of CSAs A. The large export ratio of CSAs B is mainly because of predominance (81%) of paddy fields, which have a large export ratio of 0.95. The paddy fields contribute 42.9% of the watershed phosphorus loss due to their large area, while their export rates per unit area are less than the average values for the CSAs B. This indicates that targeting paddy fields would be less efficient than focusing on other land types in the CSAs B, but may not be avoided if water quality conservation was a high priority. In the latter case, pollution control for paddy fields must focus on reducing fertilizer and manure input, as well as in retaining phosphorus during the delivery process. Best management practices such as grassed waterway, detention pond, and reuse of drainage water for irrigation are recommended. The residential areas in CSAs B have larger export ratio than those in CSAs A, which indicates that control of the delivery process is also necessary in these areas.

4. Discussion

4.1. STEM-P capacity and perspective for NPS pollution control

A spatially and temporally distributed NPS pollution model, STEM-P was developed to simulate phosphorus export from each pixel in a landscape contributing phosphorous-contaminated runoff to a water body. It proved to satisfy the three objectives for accurate and cost-effective management as proposed in the introduction part. First, the model performance in simulating phosphorus was demonstrated to be good with visual graphs of time series and statistics. Second, simulated results were reported on a grid-cell basis (Fig. 5 and Fig. 6), so that field or sub-field CSAs were identified to facilitate pollution control decisions (Fig. 6). Third, the flow paths and the travel time of surface runoff were accounted for in simulating the phosphorus delivery process (Eq. (5)), and the flow paths can be delineated (Fig. 5) to assist in the design and placement of delivery-specific remediation practices, such as vegetation buffer strips, grassed waterways, detention ponds, and artificial wetlands. The STEM-P is therefore suitable for the selection and placement of watershed-scale and field-scale conservation practices.

The CSAs in the case study were defined based on the mean and standard deviation values of the annual exported phosphorus load across the watershed, which did not account for the water quality standards. The current criteria for CSAs may be too low to meet the water quality standard or too high, thus being more costly than it is necessary. A better method of defining CSAs would first quantify the gap between current conditions and the water quality standards, and set the goal of load reduction accordingly. Then, CSAs would be defined based on the load reduction goal and the estimated potential of phosphorus loss reduction on these CSAs. This method may require techniques such as optimization and artificial intelligence that have recently been applied in sustainability and water resource management (Muttil and Chau, 2007; Wu et al., 2010). More importantly, accurate estimation of phosphorus loss reduction requires assessment of specific management practices, an important capacity that the current STEM-P does not provide.

Some mature NPS models such as L-THIA and STEPL incorporate a module to assess best management practices (BMPs) after years of development (Liu et al., 2015; Park et al., 2014). The STEM-P does not provide a module for BMP assessment yet, but it has the potential to assess BMPs by changing input data and parameters. Arabi et al. (2008) summarized the representation of various agricultural BMPs (contour farming, parallel terraces, cover crops, residue management, filter strips, grassed waterways, grade stabilization structures, etc.) in the SWAT model by changing parameters. This scheme can be applied in STEM-P and its hydrologic basis (DHM-WM). For instance, grassed waterways increase vegetation coverage and roughness in drainage ditches so that their delivery rate must be modified to represent the effect of the BMP. However, more controlled field experiments and model tests are necessary to quantify more accurately the effect of various BMPs on the STEM-P parameters, especially those new in STEM-P and not used in other models.

4.2. Advantage and limitations of the STEM-P model

Heathwaite (2003) suggested that empirical but process-based models are prospective solutions to balance the requirement of data and parameters and the capacity of providing detailed spatial and temporal information. Based on this idea, STEM-P focuses on the landscape processes of phosphorus transfer that were commonly ignored in current NPS models: the mobilization and delivery processes with surface runoff. In this way, STEM-P simulates mobilized phosphorus and exported phosphorus separately (Fig. 5), which facilitates calculation of some key variables (Table 5) to further analyze the critical process

Table 5
Land cover composition of the critical source areas (CSAs) and their phosphorus loss risk.

	Annual surface runoff (mm)	Average export ratio	Annual exported phosphorus per unit area (kg/km^2)	Area (km^2)	Area percentage (%)	Annual exported phosphorus (kg)	Percentage of exported phosphorus (%)
CSAs A	**586.4**	**0.85**	**514.7**	**7.95**	**3.4**	**4092**	**25.2**
Residential	748.3	0.79	648.1	4.04	1.9	2618	16.1
Orchard	408.2	0.88	370.0	2.16	1.0	799	4.9
Dry field	415.0	0.94	372.8	1.41	0.7	526	3.2
Paddy field	503.3	0.98	435.9	0.34	0.2	148	0.9
CSAs B	**331.2**	**0.91**	**243.1**	**36.98**	**17.1**	**8990**	**55.3**
Paddy field	320.5	0.95	233.4	29.90	13.8	6979	42.9
Orchard	386.0	0.68	290.8	3.11	1.4	904	5.6
Dry field	357.5	0.79	281.5	2.74	1.3	771	4.7
Residential	304.1	0.88	273.2	0.85	0.4	232	1.4
Forest	604.9	0.97	272.6	0.25	0.1	68	0.4
Grassland	597.2	0.99	271.6	0.12	0.1	33	0.2

and reason of phosphorus loss. Also, STEM-P summarizes various spatial and temporal influencing factors of phosphorus transfer with surface runoff with two parameters: the zero-order mobilization rate (m) and the first-order delivery rate (δ). This simplification largely reduces the burden from parameter calibration. There are at most 6 parameters (listed in Table 3) to calibrate if the study watershed has paddy fields. If paddy fields do not occur, there are at most 4 parameters to calibrate.

There was one monitoring station at the watershed outlet for model calibration and validation in this case study, which is a common limitation in many regions. In this case, model calibration guarantees that the overall phosphorus export is reasonable, yet the reliability of the spatial results depends on the accuracy of the input spatial data (including distributed surface-runoff depth and travel time simulated by DHM-WM in this case study) and on the quality of the determined values of the two distributed parameters (the mobilization rate (m) and the delivery rate (δ)) of STEM-P. The determination of the mobilization rates considers the most influential factor, the difference of stored phosphorus among land covers, which makes its specification less uncertain. The soil types would also impact mobilization rates. Soil erodibility impacts the content of soil particles that can be mobilized to runoff, and soil properties (such as pH and organic matter content) generally determine the existing forms of phosphorus (dissolved or solid phase) in soils (Radcliffe and Cabrera, 2006). These impacts of soil types were not represented in the current version of STEM-P for the sake of simplicity; yet, these are worthy of consideration in future research to obtain better spatial results. In addition, mobilization rates were assumed constant within simulation periods, since they are determined by the long-term storage balance in the soil surface. However, the mobilization rate on impervious lands may be more dynamic, since pollutants accumulate on no-rain days and be flushed off once during storms without a balanced process in soil profile. In this sense, the assumption of constant mobilization rate in STEM-P may be not applicable for urbanized watersheds. For delivery rates, the recommended values were based on values reported in previous research and from knowledge about phosphorus retention. It is necessary to track recent research about phosphorus delivery research and update the recommended values of delivery rates accordingly. In addition, the delivery rates are impacted by complex factors, such as surface roughness, flow velocity, vegetation density, and microbial activity. Users may need to adjust the delivery rate of one or several land types to obtain values representative of the conditions within their study areas.

STEM-P applies an average phosphorus concentration of the flooded water ($PCONC_{pddy}$) and an average phosphorus concentration of groundwater flow from flooded paddy fields ($PCONC_{gw\_pddy}$) to model phosphorous transfer from flooded paddy fields. These two parameters are assumed to be constant in the current version of STEM-P, while they vary with time in actuality. This was a key factor that reduced the model performance in simulating daily and the monthly variation of phosphorus in the Fengyu Watershed since paddy fields cover a large area. Theoretically, the phosphorus concentration of flooded water on paddy fields decreases with increasing precipitation, increases with increasing evaporation, and increases or decreases with irrigation depending on the concentration of the irrigated water. The phosphorus concentration in leaching water was found to decrease during the growing season in a purplish soil region in southern China (Li et al., 2009). However, the field of research concerning long-term continuous P concentration variations is in a nascent stage, which complicates efforts to fully understand and model the underlying governing mechanisms, and hinders the development of suitable equations for simulation. Rice production has a vital role in Asian agriculture, which justifies more long-term continuous field observations on paddy fields, the measuring of phosphorus concentrations in flooded and leaching waters, and continued research about influencing factors, such as daily precipitation, evaporation, irrigation, flooded water depth, leaching rate, and the like.

5. Conclusions

STEM-P is an initial attempt to simulate NPS pollution loss from landscapes to water bodies by representing pollutant mobilization and delivery processes using empirical functions. It bypasses the use of complex mechanistic models for phosphorous simulation, yet, it provides helpful insight about fine-scale critical source areas and runoff flow paths that can assist in the selection, design and placement of water quality conservation and pollution control practices. The constant assumption of mobilization rates makes STEM-P applicable for natural/agricultural watersheds. Temporal variation of the mobilization rate should be represented if applied in urbanized watersheds with impervious surfaces. Representing the impact of soil types on mobilization rates and the phosphorus concentration variations in paddy fields are worthy tasks for future model modifications. The application of STEM-P to watersheds of various sizes and geo-climatic characteristics, and developing a BMP assessment module are promising research endeavors.

Acknowledgements

This work was supported by the National Key Research and Development Program of China [grant number 2016YFD0800500], the National Natural Science Foundation of China [grant number 41471433], and the Youth Innovation Promotion Association CAS [grant number 2016304].

References

Alexander, R.B., Johnes, P.J., Boyer, E.W., Smith, R.A., 2002. A comparison of models for estimating the riverine export of nitrogen from large watersheds. Biogeochemistry 57 (1):295–339. http://dx.doi.org/10.1023/a:1015752801818.

Arabi, M., Frankenberger, J.R., Engel, B.A., Arnold, J.G., 2008. Representation of agricultural conservation practices with SWAT. Hydrol. Process. 22 (16):3042–3055. http://dx.doi.org/10.1002/hyp.6890.

Arnold, J.G., Srinivasan, R., Muttiah, R.S., Williams, J.R., 1998. Large area hydrologic modeling and assessment part I: model development. JAWRA J. Am. Water Resour. Assoc. 34 (1), 73–89.

Bingner, R., Theurer, F., 2001. AnnAGNPS Technical Processes: Documentation Version 2. Agricultural Research Service, US Department of Agriculture, Oxford, MS.

Buchanan, B.P., et al., 2013. A phosphorus index that combines critical source areas and transport pathways using a travel time approach. J. Hydrol. 486:123–135. http://dx.doi.org/10.1016/j.jhydrol.2013.01.018.

Chen, H., Teng, Y., Wang, J., 2013. Load estimation and source apportionment of nonpoint source nitrogen and phosphorus based on integrated application of SLURP model, ECM, and RUSLE: a case study in the Jinjiang River, China. Environ. Monit. Assess. 185 (2):2009–2021. http://dx.doi.org/10.1007/s10661-012-2684-z.

Chescheir, G.M., Gilliam, J.W., Skaggs, R.W., Broadhead, R.G., 1991. Nutrient and sediment removal in forested wetlands receiving pumped agricultural drainage water. Wetlands 11 (1), 87–103.

Davis, J.R., Koop, K., 2006. Eutrophication in Australian rivers, reservoirs and estuaries–a southern hemisphere perspective on the science and its implications. Hydrobiology 559 (1), 23–76.

Duchemin, M., Hogue, R., 2009. Reduction in agricultural non-point source pollution in the first year following establishment of an integrated grass/tree filter strip system in southern Quebec (Canada). Agric. Ecosyst. Environ. 131 (1–2):85–97. http://dx.doi.org/10.1016/j.agee.2008.10.005.

Gburek, W.J., Sharpley, A.N., Heathwaite, L., Folmar, G.J., 2000. Phosphorus management at the watershed scale: a modification of the phosphorus index. J. Environ. Qual. 29 (1), 130–144.

Ghebremichael, L.T., Veith, T.L., Hamlett, J.M., 2013. Integrated watershed- and farm-scale modeling framework for targeting critical source areas while maintaining farm economic viability. J. Environ. Manag. 114:381–394. http://dx.doi.org/10.1016/j.jenvman.2012.10.034.

Gu, L.Z., Wu, D.L., Hao, S.Y., 1991. Quantitative research of non-point source pollution from agricultural fields in Dianchi Lake watershed (in Chinese). Yunnan Environ. Prot. 2, 11–19.

He, F., 2015. Characteristics of phosphorus loss and the controlling strategy for vegetation restoration in phosphorus enriched area in Lake Dianchi watershed, China. Thesis (Ph.D.). Yunnan University.

Heathwaite, A.L., 2003. Making process-based knowledge useable at the operational level: a framework for modelling diffuse pollution from agricultural land. Environ. Model. Softw. 18 (8–9):753–760. http://dx.doi.org/10.1016/s1364-8152(03)00077-x.

Heathwaite, A.L., et al., 2003. The Phosphorus Indicators Tool: a simple model of diffuse P loss from agricultural land to water. Soil Use Manag. 19 (1):1–11. http://dx.doi.org/10.1079/sum2002174.

Hesse, C., Krysanova, V., Vetter, T., Reinhardt, J., 2013. Comparison of several approaches representing terrestrial and in-stream nutrient retention and decomposition in watershed modelling. Ecol. Model. 269:70–85. http://dx.doi.org/10.1016/j.ecolmodel.2013.08.017.

Johnes, P.J., 1996. Evaluation and management of the impact of land use change on the nitrogen and phosphorus load delivered to surface waters: the export coefficient modelling approach. J. Hydrol. 183 (3–4):323–349. http://dx.doi.org/10.1016/0022-1694(95)02951-6.

Lemunyon, J., Gilbert, R., 1993. The concept and need for a phosphorus assessment tool. J. Prod. Agric. 6 (4), 483–486.

Li, X.P., Li, J.L., Shi, X.J., 2009. Phosphorus leaching from rice-wheat rotation fields and its impact on groundwater (in Chinese). Proceedings for Chinese Society of Environmental Sciences 2009, p. 1.

Li, S., Gitau, M., Engel, B.A., Zhang, L., Du, Y., Wallace, C., Flanagan, D.C, 2017a. Development of a distributed hydrologic model for watershed management. Hydrol. Sci. J. http://dx.doi.org/10.1080/02626667.2017.1351029.

Li, S., Gitau, M., Bosch, D., Engel, B.A., Zhang, L., Du, Y., 2017b. Development of a soil moisture-based distributed hydrologic model for determining hydrologically-based critical source areas. Hydrol. Process. http://dx.doi.org/10.1002/hyp.11276.

Lin, J.P., 2004. Review of Published Export Coefficient and Event Mean Concentration (EMC) Data (DTIC Document).

Lindström, G., Pers, C., Rosberg, J., Strömqvist, J., Arheimer, B., 2010. Development and testing of the HYPE (Hydrological Predictions for the Environment) water quality model for different spatial scales. Hydrol. Res. 41 (3–4):295–319. http://dx.doi.org/10.2166/nh.2010.007.

Liu, Y., Ahiablame, L.M., Bralts, V.F., Engel, B.A., 2015. Enhancing a rainfall-runoff model to assess the impacts of BMPs and LID practices on storm runoff. J. Environ. Manag. 147, 12–23.

Loáiciga, H.A., Sadeghi, K.M., Shivers, S., Kharaghani, S., 2015. Stormwater control measures: optimization methods for sizing and selection. J. Water Resour. Plan. Manag. http://dx.doi.org/10.1061/(ASCE)WR.1943-5452.0000503.

Ma, X., Li, Y., Zhang, M., Zheng, F.Z., Du, S., 2011. Assessment and analysis of non-point source nitrogen and phosphorus loads in the Three Gorges Reservoir Area of Hubei Province. China. Sci. Total Environ. 412:154–161. http://dx.doi.org/10.1016/j.scitotenv.2011.09.034.

Malve, O., et al., 2012. Estimation of diffuse pollution loads in Europe for continental scale modelling of loads and in-stream river water quality. Hydrol. Process. 26 (16): 2385–2394. http://dx.doi.org/10.1002/hyp.9344.

Moriasi, D.N., Gitau, M.W., Pai, N., Daggupati, P., 2015. Hydrologic and water quality models: performance measures and evaluation criteria. Trans. ASABE 58 (6), 1763–1785.

Muttil, N., Chau, K.W., 2007. Machine-learning paradigms for selecting ecologically significant input variables. Eng. Appl. Artif. Intell. 20 (6), 735–744.

Novotny, V., 1999. Diffuse pollution from agriculture—a worldwide outlook. Water Sci. Technol. 39 (3), 1–13.

Park, Y.S., Engel, B.A., Harbor, J., 2014. A web-based model to estimate the impact of best management practices. Water 6 (3), 455–471.

Radcliffe, D.E., Cabrera, M.L., 2006. Modeling Phosphorus in the Environment. CRC Press.

Roberts, W.M., Stutter, M.I., Haygarth, P.M., 2012. Phosphorus retention and remobilization in vegetated buffer strips: a review. J. Environ. Qual. 41 (2):389–399. http://dx.doi.org/10.2134/jeq2010.0543.

Sadeghi, K.M., Loáiciga, H.A., Kharaghani, S., 2017. Stormwater control measures for runoff and water quality management in urban landscapes. J. Am. Water Resour. Assoc.: 1–10 http://dx.doi.org/10.1111/1752-1688.12547.

Shen, Z.Y., Hong, Q., Chu, Z., Gong, Y.W., 2011. A framework for priority non-point source area identification and load estimation integrated with APPI and PLOAD model in Fujiang watershed. China. Agric. Water Manage. 98 (6):977–989. http://dx.doi.org/10.1016/j.agwat.2011.01.006.

Shi, Z.S., Xu, Y.B., Lei, B.K., Liu, H.B., 2013. Dynamic changes of nitrogen and phosphorus concentrations in surface waters of paddy soils in the northern area of Erhai Lake (in Chinese). Am. Eurasian J. Agric. Environ. Sci. 32 (4), 838–846.

Smith, V.H., 2003. Eutrophication of freshwater and coastal marine ecosystems a global problem. Environ. Sci. Pollut. Res. 10 (2), 126–139.

Smith, R.A., Schwarz, G.E., Alexander, R.B., 1997. Regional interpretation of water-quality monitoring data. Water Resour. Res. 33 (12):2781–2798. http://dx.doi.org/10.1029/97wr02171.

Syversen, N., 2005. Effect and design of buffer zones in the Nordic climate: the influence of width, amount of surface runoff, seasonal variation and vegetation type on retention efficiency for nutrient and particle runoff. Ecol. Eng. 24 (5):483–490. http://dx.doi.org/10.1016/j.ecoleng.2005.01.016.

Uusi-Kamppa, J., Braskerud, B., Jansson, H., Syversen, N., Uusitalo, R., 2000. Buffer zones and constructed wetlands as filters for agricultural phosphorus. J. Environ. Qual. 29 (1), 151–158.

Winter, J.G., Duthie, H.C., 2000. Export coefficient modeling to assess phosphorus loading in an urban watershed. JAWRA J. Am. Water Resour. Assoc. 36 (5):1053–1061. http://dx.doi.org/10.1111/j.1752-1688.2000.tb05709.x.

Wu, C.L., Chau, K.W., Fan, C., 2010. Prediction of rainfall time series using modular artificial neural networks coupled with data-preprocessing techniques. J. Hydrol. 389 (1–2), 146–167.